DOI: 10.31401/WS.2023.proc.01

Six EUV Solar Radiation Proxies: A Comparative Analysis

Elias A.G.[1,2], Medina F.D.[1,2], Duran T.[3,4], Zossi B.Z.[1,2], de Haro Barbas B.F.[1,2]

[1]Laboratorio de Ionosfera, Atmosfera Neutra y Magnetosfera (LIANM), Facultad de Ciencias Exactas y Tecnologia (FACET), Universidad Nacional de Tucuman (UNT), Argentina;
aelias@herrera.unt.edu.ar
[2]INFINOA (CONICET-UNT), Argentina
[3]Departamento de Física, Universidad Nacional del Sur (UNS), Bahía Blanca, Argentina
[4]Instituto de Física del Sur (CONICET-UNS), Bahía Blanca, Argentina

Abstract.

Six EUV solar radiation proxies (Mg II, Lyman alpha flux, F10.7, Rz, F30 and He II) are analyzed along the period 1979-2022, covering four solar activity cycles, to assess their differences and similarities along the different phases of the quasi-decadal cycle. Following a previous study based on four of these proxies, their variability is compared through: (1) a correlation analysis, (2) their sensitivity along the solar activity cycle through its variation in terms of percentage, and (3) their role in filtering the solar activity effect from ionospheric F2 region critical frequency, foF2. The differences detected through these approaches can be used to decide which solar proxy to use according to the research purpose.

Keywords: solar proxy; EUV solar indices; solar activity cycle; foF2 trends.

Introduction

In this study, we aim to explore two issues: how different solar EUV proxies behave, and how well do they represent solar EUV radiation for ionospheric studies. Based on two previous studies [Elias et al., 2021; Elias et al., 2023], and on the works by Bruevich et al. [2014] and Bruevich and Bruevich [2019], we make a comparative analysis of six EUV solar radiation proxies: Mg II, Lyman α, F10.7, Rz, F30, and He II along the period 1979-2022 which covers four solar activity cycles. Among the several statistical methods available for this purpose we choose a correlation analysis and a sensitivity evaluation along the different solar cycle phases. In addition, we compare these proxies' ability to filter out solar EUV variability effect on the critical frequency of the F2-layer of the ionosphere, foF2. This parameter is a measure of the peak electron density of the ionosphere and is highly sensitive to solar EUV variations.

Data

Six solar activity proxy were considered, that is we added two proxies to the four already analyzed in our previous works [Elias et al., 2021; Elias et al., 2023]:

(1) MgII core-to-wing ratio (MgII), which corresponds to the ratio of the h and k lines of the solar MgII emission at 280 nm to the background solar continuum near 280 nm. The composite MgII was used, which combines data from different satellites. It is available from the University of Bremen [Snow et al., 2014] (https://www.iup.uni-bremen.de/UVSAT/datasets/mgii).

(2) Lyman α flux (Fα) (in W/m^2), which corresponds to the full disk integrated solar irradiance over 121-122 nm, and is dominated by the solar HI 121.6 nm emission. The composite Fα was used, which combines multiple instruments and models, available from the Laboratory for Atmospheric and Space Physics (LASP, University of Colorado) Interactive Solar Irradiance Data Center (LISIRD) [Machol et al., 2019].

(3) F10.7 (in sfu=10^{-22}Ws/m^2), which corresponds to the radio emission from the Sun at 10.7 cm (2800 MHz), and is measured at the Earth's surface at the Penticton Radio Observatory in

British Columbia, Canada (https://www.spaceweather.gc.ca/forecast-prevision/solar-solaire/solarflux/sx-5-en.php).

(4) The sunspot number (Rz), from the revised Rz data base obtained from SILSO (Sunspot Index and Long-term Solar Observations), Royal Observatory of Belgium, Brussels (https://www.sidc.be/SILSO/datafiles).

(5) F30 (in sfu=10^{-22}Ws/m^2), which corresponds to the radio emission from the Sun at 30 cm (1GHz), and is available at the National Astronomical Observatory of Japan (http://solar.nro.nao.ac.jp/norp/html/daily_flux.html).

(6) HeII (in 10^{11} ph/cm^{2}s) which corresponds to solar flux at 30.4 nm, and is available at http://projects.pmodwrc.ch/solid-visualization/makeover/index.php until 2015 and updated to 2022 from https://lasp.colorado.edu/lisird/data/soho_sem_P1D.

MgII, Fα, F30 and HeII monthly means were estimated from their daily data base, while F10.7 and Rz monthly values were directly obtained from their data source. The period January 1979-December 2022 is considered. In terms of their solar origin, they are from: the photosphere for Rz, the higher chromosphere for MgII, the transition region to the corona for Fα, the higher chromosphere and the corona for F10.7 and F30, and the transition region for HeII.

foF2 data from 9 stations, listed in Table 1, at 12 LT were used. Monthly median foF2 data were obtained as follows. Japanese and Australian stations data are available from the National Institute of Information and Communications Technology, Japan (https://wdc.nict.go.jp/IONO/index_E.html) and the World Data Centre (WDC) for Space Weather, Australia (https://downloads.sws.bom.gov.au/wdc/iondata/au/), respectively. European stations monthly medians up to 2009 were obtained from Damboldt and Suessman database [Damboldt and Suessman, 2012] (https://downloads.sws.bom.gov.au/wdc/iondata/medians/). In the case of Juliusruh, the period was updated until 2022 from https://www.ionosonde.iap-kborn.de/mon_fof2.htm. In the case of Boulder and Rome the period was updated from Lowell GIRO Data Center (LGDC) [Reinisch and Galkin, 2011].

Table 1. Geographic coordinates and geomagnetic latitude of the 9 ionospheric stations analyzed

Station	Geographic Latitude [°]	Geographic Longitude [°]	Geomagnetic Latitude [°]
Okinawa	26.31	127.59	17.28
Wakkanai	45.25	141.40	37.06
Kokubunji	35.71	139.49	27.28
Canberra	-35.17	149.08	-41.74
Townsville	-19.16	146.48	-26.21
Hobart	-42.53	147.19	-49.22
Juliusruh	54.60	13.40	53.98
Boulder	40.13	-105.23	47.65
Rome	41.54	12.29	41.49

Correlation analysis

In Table 2 the squared correlation coefficients, r^2, which indicates the variance explained between each pair of EUV proxies considering annual mean series are listed. It can be noticed that all are greater than 0.94, which means that there is 94% of common variance between all of them, except the case between HeII and Fα. So we could say, at least statistically, that they have a common forcing, which we also assume is the same as for the EUV radiation.

When we correlate annual series of each month, without any averaging, the correlation decreases. In Fig. 1, as an example, we have r^2 between each EUV proxy and Mg II for each month along the period 1979-2022. The dashed line indicates the correlation for the annual mean series, which is clearly higher than almost every monthly correlation.

We also repeated the running correlation analysis, as in Elias et al. [2021], based on the work by Bruevich et al. [2014] in order to go through the different phases of the solar cycle, considering a 3-year window for each of the solar EUV proxy pairs. The results, with the addition of F30 and HeII in the present work, are the same to those shown in Fig. 1 of Elias et al. [2021]. The correlation decreases for maximum and minimum periods in all the cases.

Table 2. Squared correlation coefficient, r^2, between each pair of the 6 solar proxies considered, for the period 1979-2022, annual series.

	Mg II	Lyman α	F10.7	Rz	F30	He II
Mg II	1					
Lyman α	0.987	1				
F10.7	0.984	0.970	1			
Rz	0.974	0.959	0.987	1		
F30	0.987	0.982	0.987	0.974	1	
He II	0.940	0.935	0.962	0.974	0.941	1

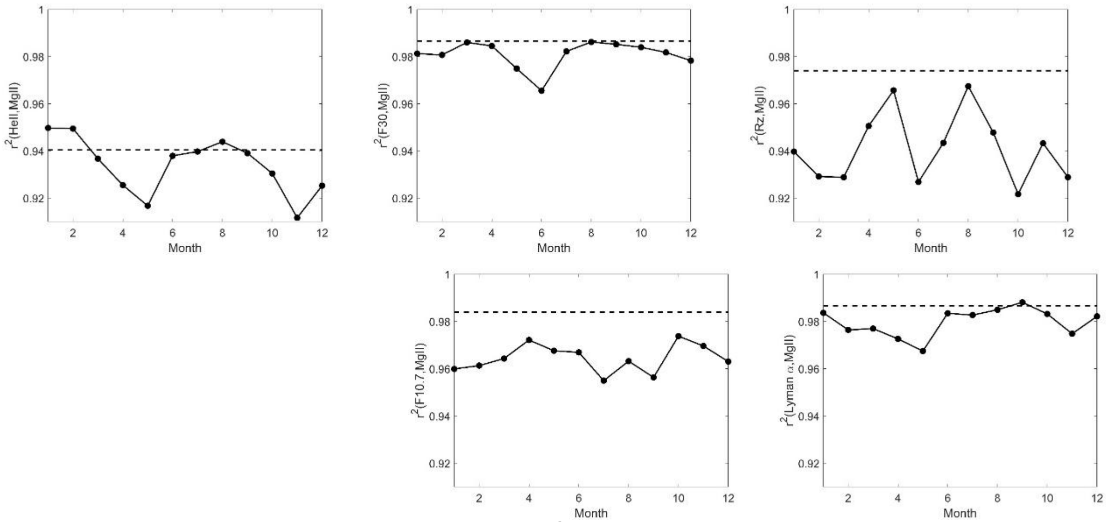

Figure 1. *Squared correlation coefficients, r^2, for time series corresponding to each month separately, for the period 1979-2022, between MgII and each of the other 5 solar EUV proxies. The dashed line indicates r^2 for the annual time series.*

Sensitivity analysis

Each proxy sensitivity along the solar activity cycle through its variation in terms of percentage was assessed as in Elias et al. [2023], adding F30 and HeII to the analysis. The amplitude of the decadal cycle relative to the mean value considering the corresponding cycle was estimated as $100 \times [X(\max) - X(\min)]/\mathrm{mean}(X)$, where X represents each EUV proxy, and $X(\max)$ and $X(\min)$ correspond to the maximum and minimum value, respectively, for each cycle, as is shown schematically in Fig. 2 in the case of Rz. In this way, sensitivity is interpreted as the response of the proxy to the variation between the maximum and the minimum level of solar activity. From highest to lowest, the average percentage sensitivity was ~250% for Rz, ~140% for HeII, ~120% for F10.7, ~110% for F30, ~45% for Fα, and 10% for MgII. The two extreme cases are Rz, for which the amplitude of variation in a cycle was two and a half times that of its average value, and MgII, for which this amplitude was of the order of one tenth of its average value.

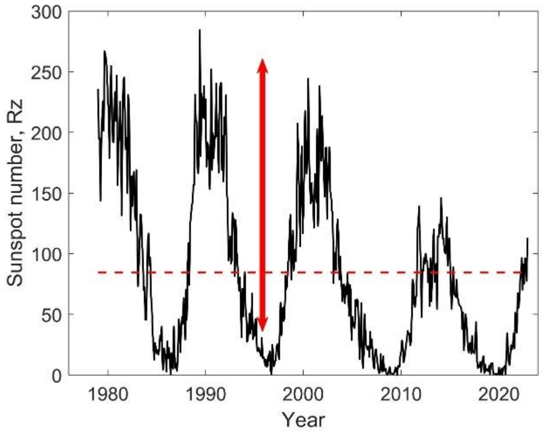

Figure 2. *Rz monthly mean series (black solid line), mean value along the period 1979-2022 (red dashed line) and amplitude from minimum to maximum of a complete cycle (red arrow).*

Trend analysis

Considering that foF2 long-term trends variability can be a "thermometer" of a solar index efficiency as an EUV proxy, we include an foF2 trend analysis as an additional characterization of the time behavior of each proxiy here analyzed. foF2 is a measure of the maximum ionospheric electron density and depends directly on solar EUV radiation, which is the main ionization source, especially at mid and low-latitudes. A key aspect of long-term trend assessments in ionospheric parameters is the solar activity filtering prior to the trend estimation. The foF2 filtering was done in the usual way by estimating the residuals from a linear regression between foF2 and each EUV proxy [Lastovicka, 2021] as follows:

$$\text{foF2 residual} = \text{foF2}_{exp} - (A\ X + B) \tag{1}$$

where foF2_{exp} is the measured foF2 data, *X* stand for the solar proxy (Rz, F10.7, MgII, Fα, F30 or HeII), and A and B are the least squares parameters of the linear regression between foF2_{exp} and X. Then, the linear trend is estimated from the linear regression between these residuals and time, that is

$$\text{foF2 residual} = \alpha\ t + \beta \tag{2}$$

where α is the desired trend in [MHz/year].

Long term trends in foF2, specifically decreasing trends, are expected due to increasing greenhouse gases concentration such as CO_2. This expected effect, however, is very small. Not more than 4%, or less, of foF2 variability, and that is why the filtering process is extremely important. Suspecting that not all EUV indices are equally efficient in representing solar EUV we estimate foF2 trends using each EUV proxy in the filtering process. It is assumed that trend values or variability patterns can show proxies' adequacy in representing EUV.

Fig. 3 shows the 9 stations' trends for each month and also for the annual means. It can be clearly seen that not all annual trends are equal. Furthermore, trends' monthly variation, even though quite similar in all the cases, are not exactly the same. Starting from the fact that all EUV proxies explain 95% or more of foF2 variance, there different possible interpretations to distinguish each proxy efficiency. If the expected trend is an foF2 decrease due to the increase in greenhouse gases concentrations, then one could argue that the proxy that best reflects EUV behavior is the one that yields negative trends. Another possibility is to assume that the best proxy is the one that yields lower trends regardless of the sign. Based on the first reasoning, HeII appears to be the least suitable reflecting the true behavior of solar EUV, even though its corresponding wavelength falls within the EUV range that ionizes the F2 layer. According to the second reasoning, the best proxies would be Rz or F10.7, contrary to the results of recent publications that favor MgII and F30 [Lastovicka and Buresova, 2023; Zossi et al., 2023]. In fact, the differences are so small, that a deeper analysis should be made in order to clearly determine which index is the best EUV measure.

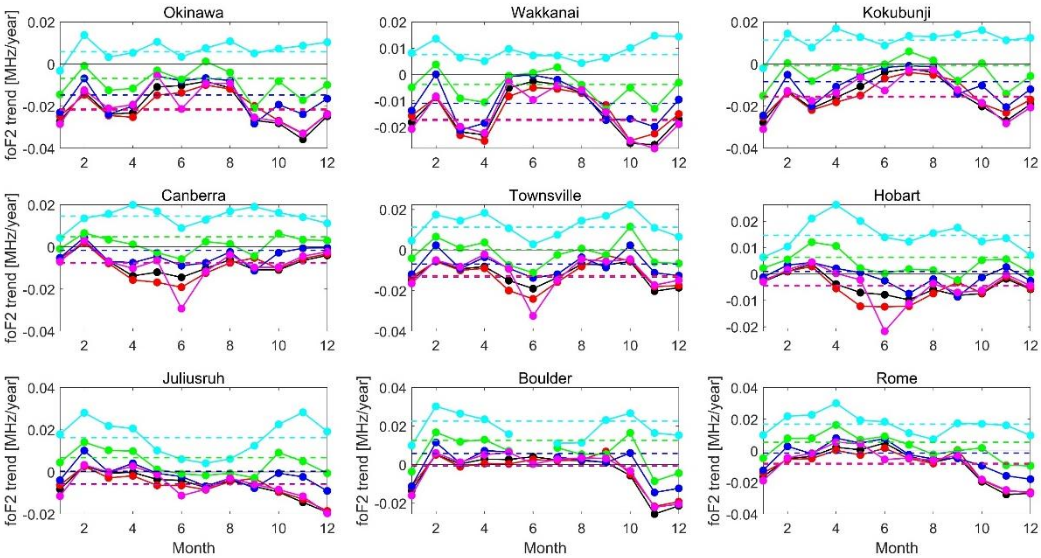

Figure 3. *foF2 trends along 1979-2022 for each month time series, filtering solar activity with MgII (black), Fα (red), F10.7 (blue), Rz (green), F30 (magenta) and HeII (cyan). Dashed lines correspond to foF2 trend assessed with annual mean values.*

Discussion and conclusions

Correlation coefficients between any pair of solar EUV proxies for the entire period 1979-2020 is greater than 0.94 but if we focus on monthly data or on shorter periods, it decreases. In monthly scales, each EUV proxy has a different source, and evidently in monthly timescales they do not have the same variation, as it is the case in annual timescale. In the case of correlation along periods shorter than the solar cycle, specifically during maximum and minimum periods when the correlation decreases, a reason could be purely statistical, as explained in Elias et al. [2021; 2023], being due to the EUV varies too little during minimum and maximum and the only variation left is the noise, which of course is not correlated with anything. Regarding each proxy sensitivity, they are all different, and probably this could explain the behavior along the last two solar minima periods which are not reflected equally by all the proxies: some are much lower than the previous minima and others present similar activity levels among all minima periods. we point this out as an important aspect that deserves a deeper research.

Going to the trend results, the difference observed in foF2 trend values, depending on which EUV proxy is used in the filtering process previous to trend calculation, may indicate their different ability to adequately represent solar EUV time variation. A possibility would be to assume that the proxy that gives smallest trends is the more adequate, or the proxy that gives the expected negative trends globally. Under both hypothesis, HeII seems to be the less adequate. Another problem here is again, the last two minima levels. If they are really lower than the previous ones, and the proxy does not show this behavior, foF2 trend will be systematically negative. This is another aspect of EUV proxies, and also of ionospheric trends' study, that deserves a much deeper research (we would like to note that there are many papers in this last years dealing with this trend problem, being still controversial).

To conclude, we wish to emphasize the significance of this analysis. The solar irradiance in the EUV spectral range is a key parameter for aeronomy and for space weather [Dudok de Witt et al., 2008]. However, it is a long-standing issue the lack of continuous observations and their limited time span. This is due to EUV measurements must be carried out above the terrestrial atmosphere, along with significant sensitivity changes of space-borne EUV detectors during long-term periods due to instrument degradation. Therefore, it is of great importance to study how different solar EUV proxies behave and how well they represent solar EUV variability, not only for ionospheric studies but for other research purposes as well.

References

Bruevich, E., Bruevich, V. (2019). Long-term trends in solar activity. Variations of solar indices in the last 40 years. Res. Astron. Astrophys., 19, 090, DOI:10.1088/1674-4527/19/7/90

Bruevich, E.A., Bruevich, V.V., Yakunina, G.V. (2014). Changed relation between solar 10.7-cm radio flux and some activity indices which describe the radiation at different altitudes of atmosphere during cycles 21–23. J. Astrophys. Astron., 35, 1–15, DOI:10.1007/s12036-014-9258-0

Damboldt, T., Suessmann, P. (2012). Consolidated Database of Worldwide Measured Monthly Medians of Ionospheric Characteristics foF2 and M(3000)F2. INAG (Ionosonde Network Advisory Group) Bulletin 73 https://www.ursi.org/files/CommissionWebsites/INAG/web-73/2012/damboldt_consolidated_database.pdf.

Dudok de Wit, T., Kretzschmar, M., Aboudarham, J., et al. (2008), Which solar EUV indices are best for reconstructing the solar EUV irradiance? Adv. Space Res., 42, 903– 911, DOI:10.1016/j.asr.2007.04.019.

Elias, A. G., de Haro Barbas, B. F., Medina, F. D., Zossi, B. S. (2021). On the correlation between EUV solar radiation proxies and their long-term association. In Proceedings of the Thirteenth Workshop “Solar Influences on the Magnetosphere, Ionosphere and Atmosphere” (pp. 20–23). Sofia, Bulgaria.

Elias, A. G., Martinis, C. R., de Haro Barbas, B. F., Medina, F. D., Zossi, B. S., Fagre, M., Duran, T. (2023). Comparative analysis of extreme ultraviolet solar radiation proxies during minimum activity levels. Earth Planet. Phys., 7, 540–547, DOI:10.26464/epp2023050

Lastovicka, J. (2021). What is the optimum solar proxy for long-term ionospheric investigations? Adv. Space Res., 67, 2-8, DOI:10.1016/j.asr.2020.07.025.

Lastovicka, J. Buresova, D. (2023). Relationships between foF2 and various solar activity proxies, Space Weather, 21, e2022SW003359, DOI:10.1029/2022SW003359.

Machol, J., Snow, M., Woodraska, D., Woods, T., Viereck, R., Coddington, O. (2019). An improved Lyman-alpha composite. Earth Space Sci., 6, 2263–2272, DOI:10.1029/2019EA000648.

Reinisch, B.W. and Galkin, I.A. (2011). Global ionospheric radio observatory (GIRO), Earth Planets and Space 63, 377-381, DOI:10.5047/eps.2011.03.001.

Snow, M., Weber, M., Machol, J., Viereck, R., Richard, E. (2014). Comparison of Magnesium II core-to-wing ratio observations during solar minimum 23/24. J. Space Weather Space Clim., 4, A04, DOI:10.1051/swsc/2014001.

Zossi, B.S., Medina, F.D., Tan Jun, G., Lastovicka, J., Duran, T., Fagre, M., de Haro Barbas, B.F., Elias, A.G. (2023). Extending the analysis on the best solar activity proxy for long-term ionospheric investigations, Proc. R. Soc. A., 479, 202302252, DOI:10.1098/rspa.2023.0225.